Effect of aspect ratio on higher order moments of velocity fluctuations in hydraulically rough open channel flow

Minakshee Mahananda[1,*], and *Prashanth* Reddy Hanmaiahgari[2]

[1]Research Scholar, Department of Civil Engineering, IIT Kharagpur, Kharagpur, India, 721302
[2]Asst. Professor, Department of Civil Engineering, IIT Kharagpur, Kharagpur, India, 721302

Abstract. The effect of aspect ratio on the higher order statistics of velocity fluctuations in a hydraulically rough turbulent open channel flow is investigated. In this regard, an experiment was conducted in a rough bed narrow open channel flow of aspect ratio equal to three and the instantaneous flow velocities were measured using a Nortek Vectrino+ Acoustic Doppler Velocimeter. To understand the effect of aspect ratio, the results obtained from the present study are compared with the literature data of approximately same Reynolds number and bed roughness in a wide open channel flow for turbulence intensities and higher order statistics of velocity fluctuations. Comparison of turbulence intensities between Narrow OCF and Wide OCF shows occurrence of higher streamwise and vertical turbulence intensities in the outer region of Narrow OCF. The results of third order moments of velocity fluctuations are sensitive to aspect ratio in the outer region.

1. Introduction

An open channel flow can be classified as either narrow or wide channel based on the aspect ratio of flow, which is defined as the ratio of the width of the channel to the depth of the flow. In a narrow channel where the ratio of width (b) of the channel to the depth of the flow (h) is less than five, strong secondary circulations such as stronger free surface vortex and a comparably weaker bottom vortex were observed while in a wide channel($b/h > 10$) secondary currents were observed only near the sidewalls but its effect is totally absent in the central region of the channel. The stronger free surface vortex in a narrow channel transports energy and momentum from the sidewall towards the channel centerline near the free surface region. As the momentum is transported from the sidewalls to the channel center, a strong downward motion takes place at the channel center and the velocity retardation causes velocity dip in the narrow open channel flow (denoted as Narrow OCF). Hence, the secondary currents have important effects on mean velocity, bed shear stresses, shear velocity, and higher order statistics of turbulent components which are important parameters for the sediment transport.

* Corresponding author: minakshee.m@iitkgp.ac.in

Turbulent components are always correlated with each other in time and space. Hence, to obtain more detailed information on turbulence characteristics, consideration of higher order statistics of velocity fluctuations is essential [1]. However, regardless of various investigations on open channel flows, the data on higher order correlations of velocity fluctuations is relatively limited [2, 3]. The higher order correlations of velocity fluctuations contain important information like coherent structures which can be described by diffusion and flux of turbulence generated Reynolds stresses [4]. Considering u', v' , and w' as the streamwise velocity fluctuations, transverse velocity fluctuations and vertical velocity fluctuations respectively, in hydrodynamics $\overline{u'u'u'}/u_{rms}^3 (= M_{30})$ defines the streamwise flux of streamwise Reynolds normal stress (RNS) skewness of the streamwise velocity fluctuations, $\overline{w'w'w'}/w_{rms}^3 (= M_{03})$ defines the vertical flux of vertical RNS or skewness of the vertical velocity fluctuations, $\overline{u'w'w'}/u_{rms}w_{rms}^2 (= M_{12})$ defines the streamwise diffusion of vertical RNS and $\overline{w'u'u'}/w_{rms}\,u_{rms}^2 (= M_{21})$ defines the vertical diffusion of streamwise RNS [6], where $u_{rms}\left(=\sqrt{\overline{u'u'}}\right)$ defines the streamwise turbulence intensity and $w_{rms}\left(=\sqrt{\overline{w'w'}}\right)$ defines as the vertical turbulence intensity. Third-order correlations of velocity fluctuations retain their signs positive or negative and deliver valuable stochastic facts. The skewness factor describes the asymmetry in pdf (probability density function) of turbulent fluctuations and it is used to explore the bursting events. The skewness of a distribution equal to zero indicates the Gaussian distribution and, other than zero that is either positive or negative indicates a temporal asymmetry of velocity fluctuations associated with bursting phenomenon. The bursting phenomenon constitutes sequences of quasi-cyclic events out of which ejections and sweep events are the most significant events. The crossover from sweep events to eject events can be identified from the point of change of sign on the third order correlations profiles [5].

In a turbulent boundary layer the third order correlations obey similarity laws with respect to different surface roughness, except in the roughness sublayer (a layer near to the wall) [6]. Although similarity exists between the turbulent boundary layer and turbulent open channel flow, but still there are important unique information which can be found out from the higher order correlations in open channel flows [2]. The effect of seepage and injection on higher order statistics of velocity fluctuations has been studied by many investigators [8, 9]. From the third-order correlations, the investigators suggested that the ejection events are predominant throughout the flow depth. In addition, the mobility of channel bed influences the higher order correlations such as by changing the diffusion of vertical RNS and the flux of streamwise RNS toward the streamwise direction and opposite in the case of rigid channel bed [10]. The investigators [10] also suggested that for the rigid channel bed, the flux of vertical RNS and the diffusion of streamwise RNS over the entire flow depth are in the upward direction and in the downward direction in the case of channel bed mobility. Mignot et al. [7] experimentally examined the structure of turbulent kinetic energy flux and shear stress over a fully rough open channel flow using acoustic Doppler velocity profiler. They have addressed the double averaging conditional statistics of shear stresses and the turbulent kinetic energy flux and also across the roughness layer, the contribution of large scale coherent structures to the turbulent kinetic energy flux. Although the aspect ratio in their study was 1.87 but the effect of aspect ratio was neglected.

From the above literature survey, it is revealed that the researchers investigated the effect of surface roughness, bed mobility and the boundary layer on the higher order turbulence statistics, but neglected the effect of flow aspect ratio (A_r) on the higher order turbulence statistics. Therefore, the objective of the present study is to examine the effect of aspect ratio on the higher order correlations of turbulent components in a turbulent narrow open channel flow.

In order to identify the effect of aspect ratio on higher order statistics of velocity fluctuations, this study has presented mean velocity profiles, Reynolds shear stress profiles and the higher order correlations profiles in a narrow open channel flow over a hydraulically rough bed. A comparison with the higher order correlation profiles and quadrants data measured by Faruque [9] in a Wide OCF over a continuous rough bed (sediment size and Reynolds number approximately equal to the present study) has been done.

2. Experimental methodology

Experiments were conducted in a 7.0 m long, 0.6 m wide, and 0.7 m deep glass-walled rectangular flume in the Hydraulic and Water Resources Engineering Laboratory at Indian Institute of Technology, Kharagpur, India. The bed slope of the flume was 0.002. Figure 1 shows a schematic diagram of the experimental facility. At the inlet to the flume, a screen is provided to make the flow stable. The bed is made of concrete with a smooth finish and clad with uniform sand particles of median diameter $d_{50} = 2.25$ mm to make it rough. Two centrifugal pumps were used to recirculate the water between the under-ground sump and the flume. The desired flow depth in the flume is achieved by adjusting the tai lgate and the flow rate is controlled by a valve located upstream of the inlet chamber. The flow depth was measured with the help of a point gauge equipped with a Vernier scale.

A three-dimensional down looking ADV system (VectrinoPlus) was used to measure the instantaneous flow velocities. The velocity measurements were taken along the centerline at the fully developed section (x = 5.15 m). Velocity measurements nearest to bed are taken at 3 mm above the bed and farthest measuring point is taken at 50 mm below the free surface. Near the bed, the velocity measurements are taken at every 0.003m, while away from the bed, the velocity measurements are taken at every 0.01 m interval and the details of coordinates are: z = 0.003, 0.005, 0.007, 0.009, 0.015, 0.02, 0.025, 0.03, 0.04, 0.05, 0.06, 0.07, 0.08, 0.09, 0.1, 0.11, 0.12, 0.13, 0.14 and 0.15 m (for flow depth 0.2 m) from the channel bed. The ADV measures instantaneous velocities at a location 50 mm below the probe emitter to minimize the influence of the probe on the measured data. The sampling rate was 100 Hz. The sampling cylinder dimensions were fixed at 6×10^{-3} m height and 6×10^{-3} m diameter. The SNR and correlation values recorded were greater than 22 and 80, respectively. The sampling duration was set to 300 s. The low frequency noise in the Vectrino raw data was despiked by using the Phase Space Threshold method as proposed by Goring and Nikora [11] and Wahl [12]. The removed spikes were replaced using a cubic interpolation method.

The aspect ratio of the flow in the present study is less than five, hence it is defined as Narrow OCF [13]. In this study, u, v and w are the time averaged streamwise, lateral and vertical velocity components, respectively; u', v' and w' are the root mean square fluctuations of corresponding velocity components; similarly $u^+ = u/u_*$, $v^+ = v/u_*$ and $w^+ = w/u_*$ are the normalized time averaged velocities and zu_*/ϑ is defined as the normalized vertical height in inner scaling where ϑ is the kinematic viscosity of water. Here, u_* is defined as the shear velocity, is obtained from the profile of the Reynolds shear stress $\left(-\overline{u'w'}\right)$ extending on to the channel boundary. Uncertainty errors in the inner layer in u and $-\overline{u'w'}$ are found to be less than 5% and 12.5%, respectively.

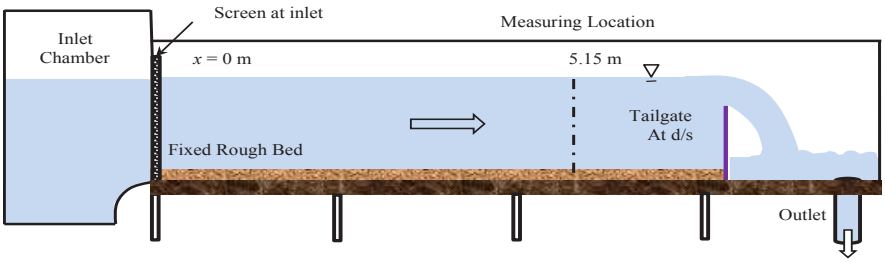

Fig. 1. A schematic diagram of experimental flume (Not to scale)

Complete experimental conditions are provided in Table 1, where U is depth averaged flow velocity in the fully developed flow region, R_e and Fr are the flow Reynolds number and the Froude number respectively. The Reynolds number is computed with length scale as the hydraulic radius. Other parameters in the Table 1, δ is the velocity dip position and Δu^+ is downward shift from the law of the wall for hydraulically smooth flow.

Table 1. Flow Conditions of Present Study and Faruque [9] Study on Continuous Rough Bed

Exp. Run	h (m)	A_r	U (m/s)	R_e	Fr	δ (m)	d_{50} (mm)	Δu^+
ER1	0.2	3	0.37	45000	0.26	0.137	2.5	7.6
Faruque (2009) Continuous Rough Bed	0.1	11	0.475	40190	0.4	-	2.46	7.7

3. Results and discussion

3.1. Inner scaling of mean velocity profiles and Reynolds shear stresses

Figures 2(a) and 2(b & c) depict the inner scaling of time averaged streamwise velocity profiles and the turbulence intensities normalized by maximum velocity respectively. The velocity distributions in the format of the law of the wall (Fig. 2a), which shows that the results of the present study follow the log-law with slight deviation in the outer region supporting the fact of the velocity dip phenomenon in Narrow OCF. The smooth wall data is represented by $u/u_* = \frac{1}{\kappa} ln(zu_*/\vartheta) + 5.0$, where u/u_* is the streamwise velocity in inner scaling, zu_*/ϑ is the vertical coordinate in inner scaling above the bed and κ is the von Karman constant which is taken as 4.1. The plot shows the downward shift in the velocity distribution of the present experiments from the smooth wall data which is consistent with Faruque [9]. Figure 2(b & c) show that the streamwise and vertical turbulence intensities higher in the outer layer in Narrow OCF as compared to Wide OCF due to the effect of aspect ratio and secondary currents.

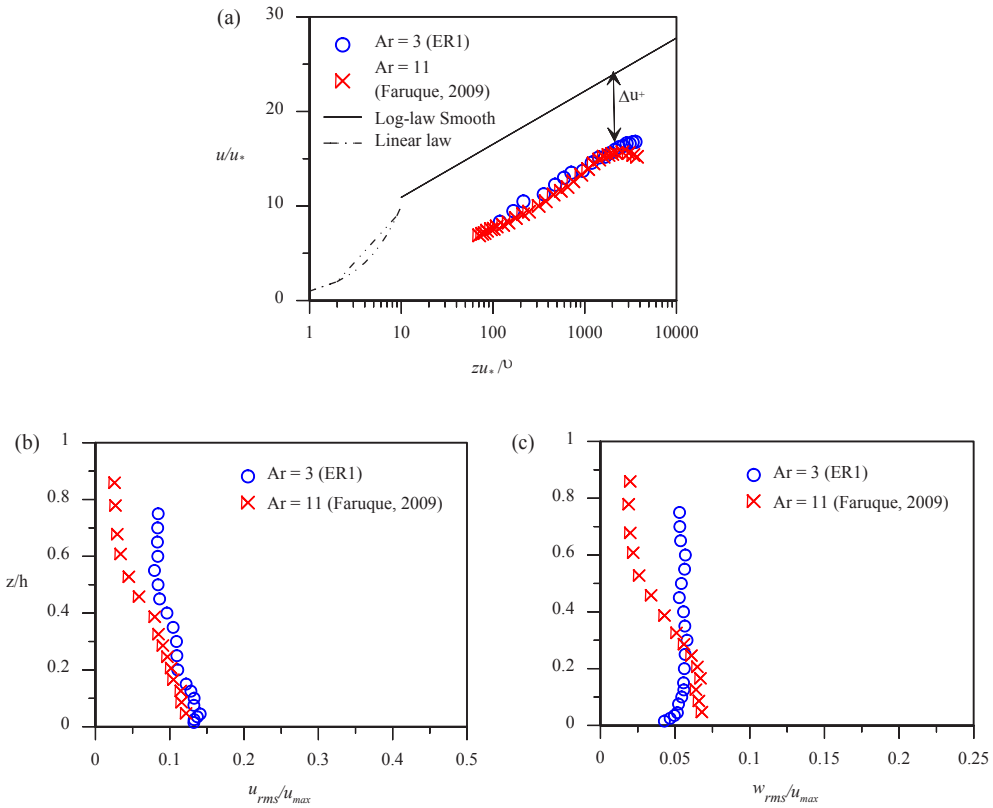

Fig. 2. (a) Vertical distribution of mean streamwise velocity of Narrow OCF (ER1) compared with the velocity profile of Wide OCF (Faruque, 2009) over a rough bed; (b) vertical distribution of streamwise turbulence intensities; (c) vertical distribution of vertical turbulence intensities of Narrow OCF (ER1) compared with Faruque (2009).

3.2. Higher order moments of velocity fluctuations

In this section, the vertical distribution of higher order moments (M_{30}, M_{03}, M_{12}, and M_{21}) are plotted for present study (Narrow OCF) and compared with the results of Faruque [9] (Wide OCF). Figures 3(a) and 3(b) represent the vertical distribution of M_{30} (streamwise flux of $\overline{u'u'}$ or skewness of streamwise velocity fluctuations) and M_{03} (vertical flux of $\overline{w'w'}$ or skewness of vertical velocity fluctuations) respectively. It is noteworthy to mention that, near the wall, the positive values of streamwise velocity fluctuations and negative values of vertical velocity fluctuations indicate sweep events. The sweep events, i.e., the inrush of high speed fluid motions from the free surface cause a positive amplitude velocity fluctuation [2]. Due to the roughness of the bed, the sweep events become stronger near the wall as shown in Fig. 3(a). It is observed in Fig. 3(a) that the vertical distributions of M_{30} in case of narrow OCF (ER1) and Wide OCF (Faruque, 2009) are collapsing on a single curve upto $z/h \approx 0.4$, but deviating afterwards with increasing z. This indicates that M_{30} is sensitive to the aspect ratio in the region $z/h > 0.4$.

Fig. 3(a) shows that streamwise flux of $\overline{u'u'}$ decreases with increasing vertical distance and attains a local negative maximum at $z/h \approx 0.4$ in case of Narrow OCF (ER1), but the negative maximum in case of Wide OCF occurs at $z/h \approx 0.69$ which shows penetration of ejection events is farther away from the wall in Wide OCF. In Narrow OCF, with further increase in vertical distance ($z/h > 0.4$), M_{30} increases (decrease in negative magnitude)

and tends to be zero at the dip position. The gradient of M_{30} variation changes at the dip position ($z_{dip}/h \approx 0.68$) and shows further decreasing trend towards the free surface ($z > z_{dip}$). From Fig. 3(a), it is evident that the negative magnitude of M_{30} for $z > 0.4$ is lesser in Narrow OCF as compared to the Wide OCF which shows higher streamwise turbulence intensities for $z > 0.4$ in Narrow OCF.

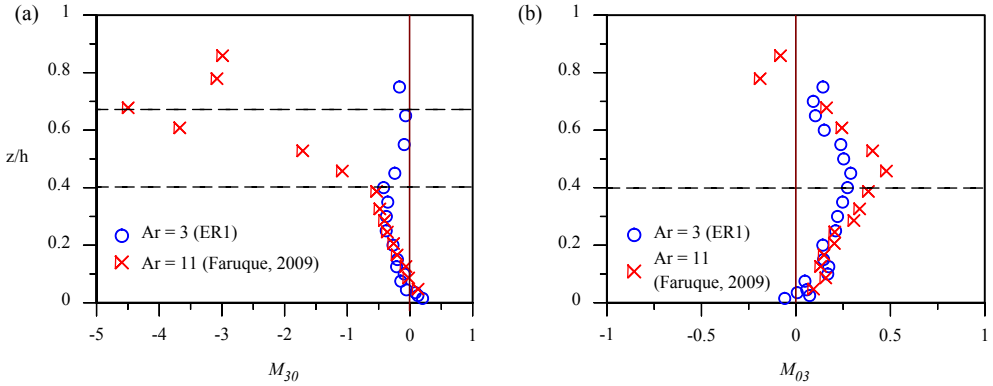

Fig. 3. (a) Vertical distribution of M_{30} of Narrow OCF (ER1) compared with M_{30} of Wide OCF (Faruque, 2009) over a continuous rough bed; (b) vertical distribution of M_{03} of Narrow OCF (ER1) compared with M_{03} of Wide OCF (Faruque, 2009) over a continuous rough bed.

Figure 3(b) depicts that the vertical flux of vertical RNS ($\overline{w'w'}$) i.e., M_{03} starts with negative values near the wall due to the sweep events and the sign changes from negative to positive at $z/h \approx 0.06$. In Narrow OCF, the positive magnitude of M_{03} increases with the increase in vertical distance for $z/h > 0.06$, and reaches a peak value at $z/h \approx 0.4$, however, M_{03} decreases with further increase in distance ($z/h > 0.4$). Similar to M_{30}, the distributions of M_{03} in Narrow OCF and Wide OCF are coinciding with each other in the region $z/h \leq 0.4$ and deviating in the outer region ($z/h > 0.4$). It is found that the minimum value of M_{30} occurs at the position close to the maximum value of M_{03}. From Fig. 3(b), it is evident that the magnitude of M_{03} for $z/h > 0.4$ is lesser in Narrow OCF as compared to the Wide OCF, which shows the occurrence of higher vertical turbulence intensities for $z/h > 0.4$ in Narrow OCF.

Figure 4(a) and 4(b) show the vertical distribution of M_{12} (streamwise diffusion of vertical RNS) and M_{21}(vertical diffusion of streamwise RNS) respectively in Narrow OCF (ER1) and comparison with Wide OCF experimental data of Faruque [9]. It is observed that in the region close to the wall ($z/h < 0.06$), the M_{12} value is positive which is consistent with the result of Keirsbulck et al. [14] for zero pressure gradient boundary layer flow. With the increase in distance from the wall ($z/h > 0.06$), the value of M_{12} becomes more negative and attains a negative peak value at $z/h \approx 0.4$. However, M_{12} magnitude in Narrow OCF (ER1) increases in magnitude as the vertical height increases for $z/h > 0.4$ towards the free surface. Wide OCF data of Faruque [9] show that the value of M_{12} attains maximum negative value at $z/h \approx 0.69$ and decreases (decrease in negative magnitude) towards the free surface ($z/h > 0.69$). Although, the M_{12} profiles of Narrow OCF and Wide OCF coinciding in the region $z/h \leq 0.4$ due to the same roughness of the bed condition, but the aspect ratio effect on M_{12} is significant in the outer region ($z/h > 0.4$).

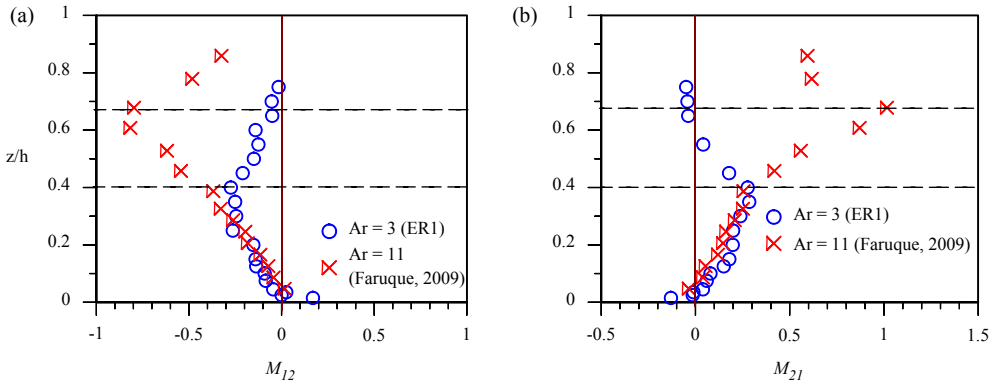

Fig. 4. (a) Vertical distribution of M_{12} of Narrow OCF (ER1) compared with M_{12} of Wide OCF (Faruque, 2009) over a continuous rough bed; (b) vertical distribution of M_{21} of Narrow OCF (ER1) compared with M_{21} of Wide OCF (Faruque, 2009) over a continuous rough bed.

Similarly Fig. 4(b) shows that the value of M_{21} starts with negative values near the wall ($z/h < 0.06$) and the sign change from negative to positive takes place at $z/h \approx 0.06$. For Narrow OCF (ER1), the value of M_{21} reach maximum at $z/h \approx 0.4$ and with further increase in vertical distance M_{21} tends decrease and attains zero in the free surface region. In contrast to the present results, the M_{21} value was attaining a maximum at $z/h \approx 0.69$ in case of Wide OCF experiment of Faruque [9]. In addition, the magnitudes of $M_{21}$and M_{21} in the region $z/h > 0.4$, are greater in Wide OCF as compared to the Narrow OCF indicating intense upward diffusion of turbulence in Wide OCF. Therefore, this deviation signifies the dominant effect of aspect ratio on M_{21}. The maximum value of M_{21} is at a position corresponds to the minimum value of M_{12} which is consistent with the results of Balachandar and Bhuiyan [2] over rough bed conditions.

From the above results, it is found that the third order statistics of velocity fluctuations are similar in the region $z/h \leq 0.4$ and the effect of aspect ratio is significant in the region $z/h > 0.4$. Near the wall region ($z/h < 0.06$), streamwise RNS flux and vertical RNS diffusion are in the streamwise direction. The streamwise RNS flux and vertical RNS diffusion are occurring against the streamwise direction and the trend become pronounced with the increase in vertical distance upto $z/h = 0.4$ in the present study. In addition, M_{21}value is positive (Fig. 3b) while the streamwise flux M_{30} (Fig. 3a) is negative, which implies a positive vertical motion and indicating strong ejection events with the upward transport of streamwise RNS away from the channel bed. However, in the region $z/h > 0.4$, the magnitudes of M_{30} and M_{21} are lesser in the present study as compared to the Wide OCF experiment of Faruque [9] because of higher streamwise and vertical turbulence intensities in Narrow OCF.

4. Conclusions

The present study was conducted to experimentally investigate the higher order statistics of velocity fluctuations in a hydraulically rough narrow open channel turbulent flow and the effect of aspect ratio on higher order moments. It is found that in the outer region, the streamwise and vertical turbulence intensities are grater in magnitude in Narrow OCF as compared to Wide OCF due to the effect of side walls in narrow open channel flow. In the region $z/h \leq 0.4$, the third order statistics collapse onto a single curve for both Narrow OCF and Wide OCF, but show a different trend in the outer region, which suggests the

distribution of flux and diffusion of RNS depends on the aspect ratio in the region away from the wall ($z/h > 0.4$). Hence, the results of third order moments of velocity fluctuations show that the effect of aspect ratio is significant in the region $z/h > 0.4$. Third order moments comparison between Narrow OCF and Wide OCF shows higher streamwise and vertical turbulence intensities for $z/h > 0.4$ in Narrow OCF.

References

1. Nezu, I., Nakagawa, H. (1993). *Turbulence in Open-Channel Flows*. *IAHR/AIRH Monograph Series*. Balkema, Rotterdam
2. Balachandar, R., Bhuiyan, F. (2007). Higher-order moments of velocity fluctuations in an open channel flow with large bottom roughness. *J. Hydraul. Eng*., **133(1)**, 77-87.
3. Cameron, S. M., Nikora, V. I., Stewart, M. T. (2017). Very-large-scale motions in rough bed open channel flow. *J. Fluid Mech*., **814**, 416-429.
4. Simpson, R., Chew, Y., Shivaprasad, B. (1981). The structure of a separating turbulent boundary layer. Part 2 : Higher-order turbulence results. *J. Fluid Mech*., **113**, 53-73.
5. Gad-el-Hak, M., Bandyopadhyay, P. (1994). Reynolds number effects in wall-bounded turbulent flows. *Appl. Mech. Rev*., **17(8)**, 307-365.
6. Raupach, M. R. (1981). Conditional statistics of Reynolds stress in rough-wall and smooth-wall turbulent boundary layers. *J. Fluid Mech*., **108**, 363-382.
7. Mignot, E., Barthelemy, E., Hurther, D. (2009a). Double-averaging analysis and local flow characterization of near-bed turbulence in gravel-bed channel flows. *J. Fluid Mech.,* **618**, 279-303.
8. Dey, S., Nath, T. K. (2010). Turbulence characteristics in flows subjected to boundary injection and suction. *J. Hydraul. Eng*., **136(7)**, 877-888.
9. Faruque, M. A. A. (2009). Smooth and rough wall open channel flow including effects of seepage and ice cover. Ph.D. Thesis, Univ. of Windsor, Canada.
10. Dey, S., Das, R. (2012). Gravel-bed hydrodynamics : Double averaging approach. *J. Hydraul. Eng*., **138(8)**, 707-725.
11. Goring, D. G., Nikora, V. I. (2002). Despiking acoustic doppler velocimeter data. *J. Hydraul. Eng*., **128(1)**, 117-126.
12. Wahl, T. L. (2003). Discussion of despiking acoustic doppler velocimeter data by Derek G. Goring and Vladimir I. Nikora. *J. Hydraul. Eng*., **129(6)**, 484-487.
13. Nezu, I., Nakagawa, H., and Tominaga, A. (1985). Secondary currents in a straight channel flow and the relation to its aspect ratio. *Turbulent Shear Flows 4*, Springer-Verlag, New York, N.Y., **4**, 246-260.
14. Keirsbulck, L., Mazouz, A., Labraga, L., Tournier, C. (2001). Influence of the surface roughness on the third-order moments of velocity fluctuations. *Exps. Fluids*, **30**, 592-594.